SARS-CoV-2 Nidoviral RNA Uridylate-Specific Endoribonuclease (NSP15)

A Target Enabling Package (TEP)

Gene ID / UniProt ID / EC	43740578 / P0DTD1 / 2.7.7.48
Target Nominator	Andre S. Godoy[1]
Collaborating Authors	Andre S. Godoy[2], Tobias Krojer[1], Aline M. Nakamura[2], Alice Douangamath[3], Gabriela D. Noske[2], Victor O. Gawrijuk[2], Rafaela S. Fernandes[2], Glaucius Oliva[2], Frank von Delft[1,3]
Target PI	Frank von Delft
Therapeutic Area(s)	Infectious diseases
Disease Relevance	NSP15 is a nidoviral RNA uridylate-specific endoribonuclease (NendoU) from SARS-CoV-2, likely involved in innate immune evasion
Date Approved by TEP Evaluation Group	November 27th 2020
Document version	1.0
Document version date	November 2020
Citation	Andre S. Godoy, Tobias Krojer, Aline M. Nakamura, Alice Douangamath, Gabriela D. Noske, Victor O. Gawrijuk, … Frank von Delft. (2020). SARS-CoV-2 Nidoviral RNA Uridylate-Specific Endoribonuclease (NSP15); A Target Enabling Package [Data set]. Zenodo. http://doi.org/10.5281/zenodo.4452937
Affiliations	[1] Centre for Medicines Discovery, Old Road Campus Research Building, University of Oxford, Roosevelt Dr, Headington, Oxford OX3 7DQ 2 Physics Institute of Sao Carlos, University of Sao Paulo, Av. Joao Dagnone, 1100, Jardim Santa Angelina, São Carlos 13563-120, Brazil. [3] Diamond Light Source Ltd., Harwell Science and Innovation Campus, Didcot, OX11 0QX, United Kingdom

SUMMARY OF PROJECT

The non-structural protein 15 (NSP15, NendoU$^{SARS-CoV-2}$) from severe acute respiratory syndrome 2 virus (SARS-CoV-2) is an uridylate-specific endoribonuclease, likely responsible in the viral immune evasion mechanism. This TEP provides a set of reagents for further interrogation of the molecular function of NSP15. We have established a purification protocol for the active protein for biochemical and structural studies. Moreover, we have crystallised the protein and performed a crystallographic fragment screen which yielded several hits. Data generated here will be used for the development of enzyme inhibitors that would illuminate the biological role of the gene product, and eventually point the way to new antiviral therapies.

SCIENTIFIC BACKGROUND

SARS-CoV-2 is the causative agent of COVID-19. NSP15 from SARS-CoV-2 is a nidoviral RNA uridylate-specific endoribonuclease that is part of the EndoU family (1). Members of the family act on RNA processing being active on both single-stranded RNA and double-stranded (ds) RNA, cleaving 3'of urydilates thereby generating a 2', 3' cyclic phosphate and 5'-hydroxyl termini (2). NSP15 domains are highly conserved amongst all nidoviruses and have not been identified in other RNA virus families, thus qualifying them as genetic markers of this order (3,4). Initially, NSP15 was thought to be required for the viral replication process, acting on viral RNA synthesis. However, studies have revealed that catalytic mutant viruses for NSP15 replicate as well as wild-type virus (5). Subsequently, it was revealed that NSP15 acts by limiting the sensing of viral RNA by the host, inhibiting the innate immune response, like type I interferon response in macrophages during viral infection by evading dsRNA sensors (such as MDA5, PKR and OAS/RNaseL) (5-7). The potential of NSP15 as a target for direct acting antiviral therapies has not been yet fully explored.

RESULTS – THE TEP

Proteins Purified

NSP15 is a346 amino acid long polypeptide of approximately 38 kDa that forms a three-domain protein. These monomers are known to self-assemble as a barrel-shaped hexamer with D3 symmetry, totalling 228 kDa. For this project, we recombinantly purified NSP15 in its monomeric form. The mechanism involved in hexamerisation *in-vitro* and *in-situ* is still under investigation.

Structure

Although recombinant protein obtained was monomeric, crystal packing revealed that NSP15 formed the expected hexamer during crystallization (**Fig 1A**). The active site of NSP15[2] was found to be in complex with citrate, which is a component of the crystallisation condition (**Fig 1B**).

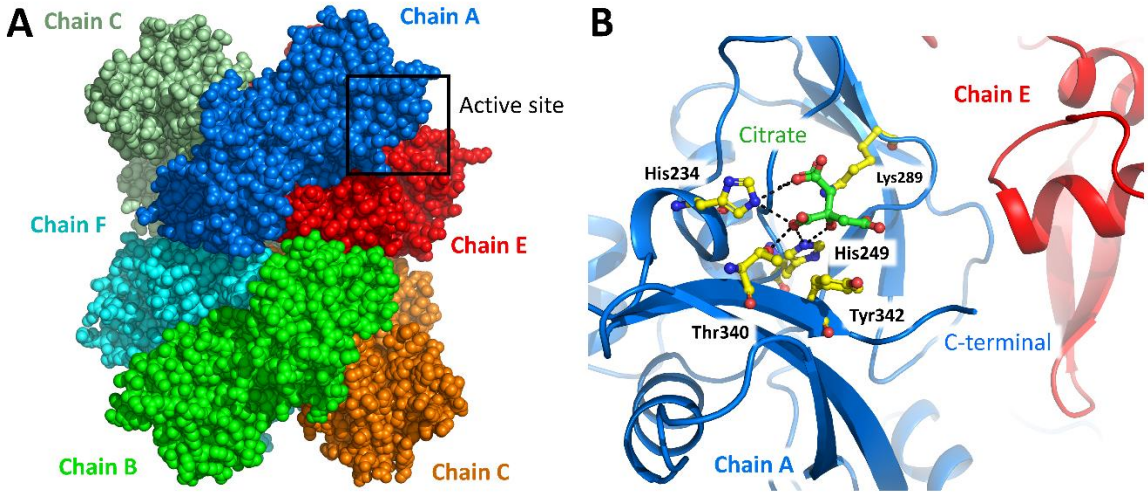

Figure 1. (A) Side-view of the barrel-shaped NSP15 hexamer depicted as spheres. Each chain is coloured with a specific colour. One of the six active sites is marked with a black square. (B) View of chain A (blue) active site. Active residues are depicted as yellow sticks. Citrate is depicted as green sticks.

Assays

We have established a fluorogenic endonuclease assay in order to be able to analyze the influence of small molecules on the activity of NSP15.

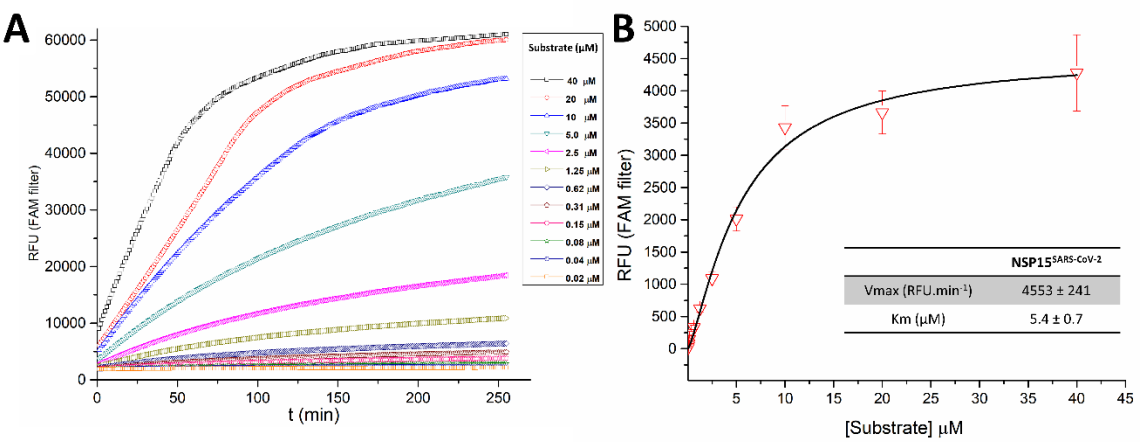

Figure 2. **(A)** Activity characterisation of NSP15. Time course reactions of NSP15 in presence of different RNA substrate concentrations. **(B)** Michaelis-Menten curve of NSP15.

Chemical Matter

The crystallographic fragment discovery campaign using the XChem platform revealed chemically distinct fragments that could bind to NSP15. Fragment screening hits were found all over the accessible NSP15 surface area (**Fig 3**). N.B.: the asymmetric unit of NSP15 crystals contains two NSP15 protomers, but some fragments were only bound to one protomer (see table below).

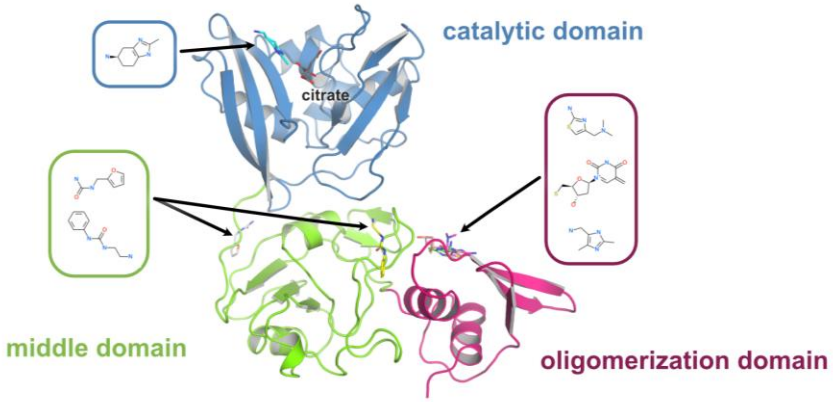

Figure 3. Overview of crystallographic fragment screening hits.

PDB ID	Ligand	Binding Location	Site	Resolution (Å)
5S6X	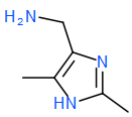	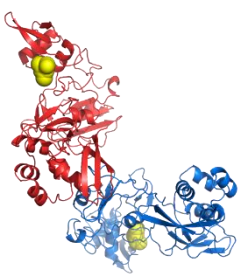	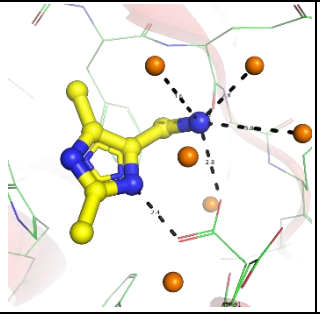	2.32

5S6Y	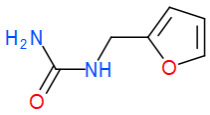	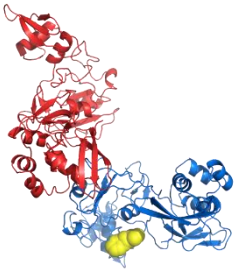	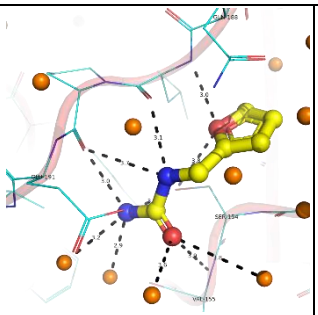	2.32
5S6Z	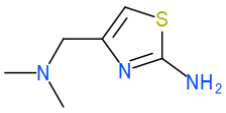	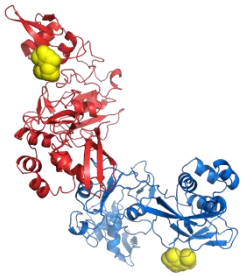	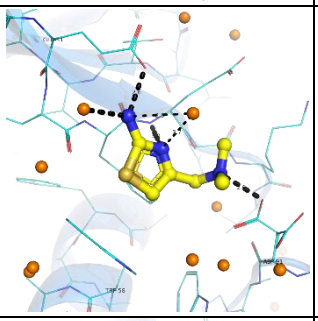	2.28
5S70	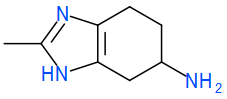	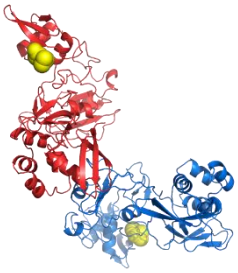	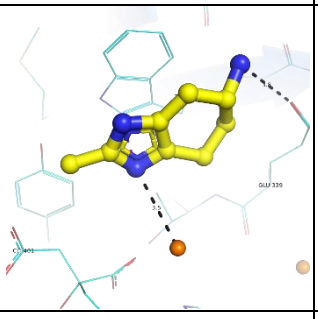	2.33
5S71	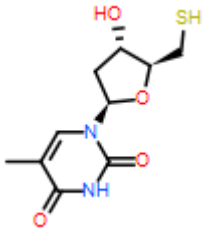	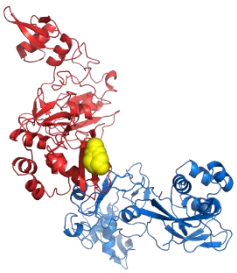	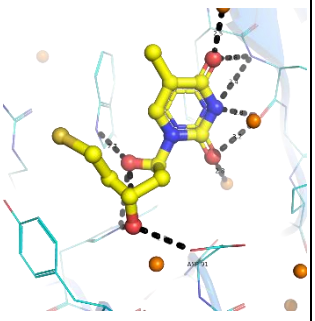	1.94
5S72	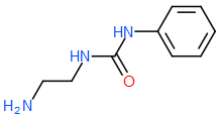	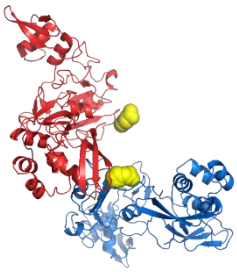	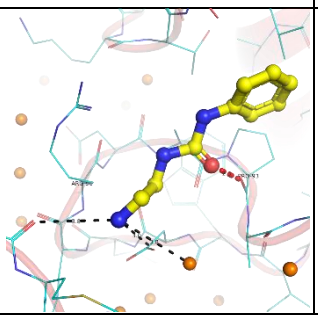	2.51

IMPORTANT: Please note that the existence of small molecules within this TEP indicates only that chemical matter might bind to the protein in potentially functionally relevant locations. The small molecule ligands are intended to be used as the basis for future chemistry optimisation to increase potency and selectivity and yield a chemical probe or lead series. As such, the molecules within this TEP should not be used as tools for functional studies of the protein, unless otherwise stated, as they are not sufficiently potent or well-characterised to be used in cellular studies.

CONCLUSION

We have produced active recombinant NSP15 protein that could be crystallised and used for structure determination at high resolution. We also obtained data from the NSP15 in complex with several fragments, which should provide valuable information for the development of a new enzyme inhibitor. Furthermore, we established a stable assay that can be used for further enzyme characterization.

TEP IMPACT

We have been working together as an international team (Brazil/ UK) for a few months only, yet have progressed a project from conception to TEP through the sharing of expertise, and by providing training in new methods (e.g. crystallographic fragment screening).
We are planning to design follow-up compounds based on the screening hits in order to obtain compounds with measurable potency, and use this as the basis to seek further funding for structure-based inhibitor development against NSP15. This is likely to proceed in collaboration with a group from EUOpenScreen.

FUNDING INFORMATION

The work performed at the SGC has been funded by a grant from the Wellcome [106169/ZZ14/Z]. This work was supported by Fundação de Amparo à Pesquisa do Estado de São Paulo (FAPESP— CEPID grant 2013/07600-3).

ADDITIONAL INFORMATION

Structure Files

PDB ID	Structure Details
5S6X	Crystal Structure of SARS-CoV-2 NendoU in complex with Z2889976755
5S6Y	Crystal Structure of SARS-CoV-2 NendoU in complex with Z56900771
5S6Z	Crystal Structure of SARS-CoV-2 NendoU in complex with PB2255187532
5S70	Crystal Structure of SARS-CoV-2 NendoU in complex with EN300-181428
5S71	Crystal Structure of SARS-CoV-2 NendoU in complex with FUZS-5
5S72	Crystal Structure of SARS-CoV-2 NendoU in complex with BBL029427

Materials and Methods

Protein expression and purification

Vector: pET28-LIC
Entry clone accession: MT126808.1
Cell line: *E. coli* BL21(DE3)
Tags and additions: N-terminal, TEV protease cleavable hexahistidine tag Construct protein sequence (underlined sequence contains vector encoded His-tag and TEV protease cleavage site*):
NendoU$^{SARS\text{-}CoV\text{-}2}$ (aa 1-346)

MKHHHHHHPMSDYDIPTTENLYFQ*GAMSLENVAFNVVNKGHFDGQQGEVPVSIINNTVYTKVDGVDVELFENKTTLPVN
VAFELWAKRNIKPVPEVKILNNLGVDIAANTVIWDYKRDAPAHISTIGVCSMTDIAKKPTETICAPLTVFFDGRVDGQVDLFR
NARNGVLITEGSVKGLQPSVGPKQASLNGVTLIGEAVKTQFNYYKKVDGVVQQLPETYFTQSRNLQEFKPRSQMEIDFLELA
MDEFIERYKLEGYAFEHIVYGDFSHSQLGGLHLLIGLAKRFKESPFELEDFIPMDSTVKNYFITDAQTGSSKCVCSVIDLLLDDFV
EIIKSQDLSVVSKVVKVTIDYTEISFMLWCKDGHVETFYPKLQ

SARS-COV2 cDNA sample was donated by Dr. Edilson Durigon (GenBank MT126808.1), generated using SCRIPT One-Step RT-PCR (Cellco Biotec) and random hexamer primers. NSP15 coding sequence was amplified using FastPol (Cellco Biotec) with primers 5'-CAGGGCGCCATGAGTTTAGAAAATGTGGCTTTTAATG-3' and 5'-GACCCGACGCGGTTATTGTAATTTTGGGTAAAATGTTTCTAC-3', and inserted pET28-LIC (gently donated by Dr. Arie Geerlof) using Ligation-Independent Cloning method (8). The final construct pET28-LIC -NSP15 included a N-terminal 6xHis-tag followed by a TEV cleaving site and residues 1-346 of NSP15.

Buffers used are detailed hereafter:
Buffer A: 50 mM TRIS-HCl pH 8.0, 300 mM NaCl, 10% glycerol, 20 mM imidazole
Buffer B: 50 mM TRIS-HCl pH 8.0, 300 mM NaCl, 10% glycerol, 300 mM imidazole
Buffer C: 20 mM HEPES pH 7.5, 150 mM NaCl, 5% (v/v) glycerol, 0.5 mM TCEP

Transformed BL21(DE3) cells were growth in LB Lennox medium supplemented with kanamycin at 37°C until DO_{600} = 1.0, and kept for 16h at 18°C after induction with 0.5 mM isopropyl β-D-1-thiogalactopyranoside. Harvested cells were resuspended in Buffer A supplemented with 0.1 mg/mLlysozyme, 10 U of benzonase (Cellco Biotec) and 1.0 mM DTT, and disrupted using sonication. Cleared lysate was passed through a HisTrap HP 5 mL (GE Healthcare) equilibrated in Buffer A, and them protein was eluted with Buffer B. Excessive imidazole was removed using a Sephadex XK 26/60 column (GE Healthcare) equilibrated with Buffer A. Sample was incubated overnight at 8°C with 4 mM DTT and 0.1 mg/mL TEV protease, then passed through a HisTrap

HP 5 mL equilibrated in Buffer A to remove non-cleaved protein and TEV protease. Final purification was performed by size exclusion chromatography using a HiLoad Superdex 75 16/60 (GE Healthcare) equilibrated with Buffer C. Purity was confirmed by SDS-PAGE 12%. Protein concentration was estimated using the theoretical extinction coefficient at 280 nm of 33,140 $M^{-1}.cm^{-1}$ (Wilkins et al., 1999). The eluted protein was pooled and concentrated to 3.4 mg/mL using a 30 kDa MWCO concentrator.

Protein crystallisation and structure determination

To crystalise NSP15, sitting drops containing 30 nL protein (3.4 mg/mL) and 30 nL well solution containing 14% (w/v) PEG 6,000 and 0.1 M Sodium Citrate pH 5.0 were equilibrated at 20 ^{o}C by vapor diffusion. Crystals were cryo-protected using 20% (v/v) ethylene glycol and flash-cooled in liquid nitrogen. Diffraction data were obtained at DLS beamlines i04.

Activity assays and kinetic analysis

Fluorogenic oligonucleotide substrate 5'6-FAM-$_{d}A_{r}U_{d}A_{d}$A-6-TAMRA3' was purchased from GenScript. Activity assays were performed in 25 mM BIS-Tris-HCl buffer 6.0 pH, 0.25 µM substrate and 100 nM $NSP15^{mon}$ at 30^{o}C. Time-curse reactions were directly monitored in a Stratagene Mx3005P (Agilent Technologies) using FAM filters

Crystallography-based fragment screening

For the fragment screening campaign, 30 nL protein (3.4 mg/mL) and 30 nL well solution containing 14% (w/v) PEG 6,000 and 0.1 M tri-sodium citrate pH 5.0 were equilibrated at 20 ^{o}C by vapor diffusion in the presence of 10 nL of seeds stocks. For soaking, 40 nL of each fragment compound from the OPEN-EU DRIVE fragment library (final concentration of 100 mM) was added to a crystallisation drop using an ECHO acoustic liquid handler dispenser at the Diamond light source XChem facility (9). Crystals were soaked for two hours before being harvested using XChem SHIFTER technology, and data was collected at the beamline I04-1 in automated mode. The XChemExplorer pipeline (10) was used for structure solution with parallel molecular replacement using DIMPLE (11). Fragments were identified using PANDDA software (12). Data was modelled and refined using BUSTER (13) and COOT (14), and validated using Molprobity (15). Coordinates and structure factors for exemplary data sets with bound fragments are deposited in the RCSB Protein Data Bank.

References

1. Kim, Y., Jedrzejczak, R., Maltseva, N. I., Wilamowski, M., Endres, M., Godzik, A., Michalska, K., and Joachimiak, A. (2020) Crystal structure of Nsp15 endoribonuclease NendoU from SARS-CoV-2. *Protein Sci* **29**, 1596-1605
2. Ulferts, R., and Ziebuhr, J. (2011) Nidovirus ribonucleases Structures and functions in viral replication. *Rna Biol* **8**, 295-304
3. Gorbalenya, A. E., Enjuanes, L., Ziebuhr, J., and Snijder, E. J. (2006) Nidovirales: Evolving the largest RNA virus genome. *Virus Res* **117**, 17-37
4. Ivanov, K. A., Hertzig, T., Rozanov, M., Bayer, S., Thiel, V., Gorbalenya, A. E., and Ziebuhr, J. (2004) Major genetic marker of nidoviruses encodes a replicative endoribonuclease. *P Natl Acad Sci USA* **101**, 12694-12699
5. Kindler, E., Gil-Cruz, C., Spanier, J., Li, Y. Z., Wilhelm, J., Rabouw, H. H., Zust, R., Hwang, M., V'kovski, P., Stalder, H., Marti, S., Habjan, M., Cervantes-Barragan, L., Elliot, R., Karl, N., Gaughan, C., Van Kuppeveld, F. J. M., Silverman, R. H., Keller, M., Ludewig, B., Bergmann, C. C., Ziebuhr, J., Weiss, S. R., Kalinke, U., and Thiel, V. (2017) Early endonuclease-mediated evasion of RNA sensing ensures efficient coronavirus replication. *Plos Pathog* **13**
6. Deng, X. F., Hackbart, M., Mettelman, R. C., O'Brien, A., Mielech, A. M., Yi, G. H., Kao, C. C., and Baker, S. C. (2017) Coronavirus nonstructural protein 15 mediates evasion of dsRNA sensors and limits apoptosis in macrophages. *P Natl Acad Sci USA* **114**, E4251-E4260
7. Hackbart, M., Deng, X. F., and Baker, S. C. (2020) Coronavirus endoribonuclease targets viral polyuridine sequences to evade activating host sensors. *P Natl Acad Sci USA* **117**, 8094-8103

8. Aslanidis, C., and Dejong, P. J. (1990) Ligation-Independent Cloning of Pcr Products (Lic-Pcr). *Nucleic Acids Res* **18**, 6069-6074
9. Collins, P. M., Ng, J. T., Talon, R., Nekrosiute, K., Krojer, T., Douangamath, A., Brandao-Neto, J., Wright, N., Pearce, N. M., and von Delft, F. (2017) Gentle, fast and effective crystal soaking by acoustic dispensing. *Acta Crystallogr D* **73**, 246-255
10. Krojer, T., Talon, R., Pearce, N., Collins, P., Douangamath, A., Brandao-Neto, J., Dias, A., Marsden, B., and von Delft, F. (2017) The XChemExplorer graphical workflow tool for routine or large-scale protein-ligand structure determination. *Acta Crystallogr D* **73**, 267-278
11. Keegan, R., Wojdyr, M., Winter, G., and Ashton, A. (2015) DIMPLE: A difference map pipeline for the rapid screening of crystals on the beamline. *Acta Crystallogr A* **71**, S18-S18
12. Pearce, N. M., Krojer, T., Bradley, A. R., Collins, P., Nowak, R. P., Talon, R., Marsden, B. D., Kelm, S., Shi, J. Y., Deane, C. M., and von Delft, F. (2017) A multi-crystal method for extracting obscured crystallographic states from conventionally uninterpretable electron density. *Nat Commun* **8**
13. Ltd., G. P. (2017) Buster. v. 2.10.13 Ed., Cambridge, United Kingdom
14. Emsley, P., Lohkamp, B., Scott, W. G., and Cowtan, K. (2010) Features and development of Coot. *Acta Crystallographica Section D-Biological Crystallography* **66**, 486-501
15. Chen, V. B., Arendall, W. B., Headd, J. J., Keedy, D. A., Immormino, R. M., Kapral, G. J., Murray, L. W., Richardson, J. S., and Richardson, D. C. (2010) MolProbity: all-atom structure validation for macromolecular crystallography. *Acta Crystallogr D* **66**, 12-21

We respectfully request that this document is cited using the DOI value as given above if the content is used in your work.